# Structurally Different Dinuclear Copper(II) Complexes with the Same Triazolopyrimidine Bridging Ligand

Mohammad Abul Haj,[a] Miguel Quirós,*[a] Juan M. Salas,[a] José A. Dobado,[b] José Molina Molina,[b][†] Manuel G. Basallote,[c] and M. Ángeles Máñez[c]

**Keywords:** Copper / N,O ligands / Metal-metal interactions / Structure elucidation

Four binuclear copper(II) compounds with the anionic form of the ligand 4,5-dihydro-5-oxo[1,2,4]triazolo[1,5-*a*]pyrimidine ($5tpO^-$) have been isolated, their formulae being $[Cu_2(5tpO)_4(H_2O)_2]\cdot 2H_2O$ (**1**), $[Cu_2(phen)_2(5tpO)_2(H_2O)_2](NO_3)_2\cdot 4H_2O$ (**2**), $[Cu_2(biim)_2(5tpO)_2(H_2O)](ClO_4)_2\cdot 5.5H_2O$ (**3**), and $[Cu_2(CH_3CO_2)_2(5tpO)_2(H_2O)_2]$ (**4**) (phen = 1,10-phenanthroline, biim = bisimidazole). A related mononuclear complex, $[Cu(phen)_2(5HtpO)_2](NO_3)_2$ (**5**), has also been prepared. The crystal structure of compounds **1**–**3** has been determined by X-ray diffraction, showing their binuclear nature with four (**1**) or two (**2**, **3**) bridging $5tpO^-$ moieties. The triazolopyrimidine ligand binds the copper atoms through N3 and N4 in compounds **1** and **3**, whereas a novel binding mode through N3 and the exocyclic oxygen atom has been found in **2**. The study of the solution behaviour of **2** and **5** shows the important role of the solvent in the formation of the mono or binuclear complex. The reduction of the metal centres to $Cu^I$ has been observed by electrochemical methods, demonstrating that this ligand stabilizes this oxidation state. Magnetic susceptibility measurements and electronic paramagnetic resonance (EPR) spectra seem to indicate a dimeric nature also for compound **4**. The antiferromagnetic interaction between the copper atoms inside the dimer is very strong for **4** ($2J = -221.3\ cm^{-1}$) and **1** ($2J = -104.9\ cm^{-1}$), fairly strong for **3** ($2J = -21.6\ cm^{-1}$), and very weak or non-existent for **2**. The nature of the copper–copper interaction in compound **1** has been analyzed by using molecular orbital calculations.

## Introduction

The study of dinuclear complexes of copper(II) is a very active research field and more than nine hundred of such complexes have been structurally characterized, according to a recent review.[1] The interaction between the spins of both metal atoms leads to the existence of two states with different energy, one with a total spin of zero (singlet) and the other with a total spin of one (triplet). This difference of energy ($2J$) is experimentally observable by means of magnetic susceptibility measurements. The value of $2J$ depends on many structural features and the Cu−Cu distance does not seem to be the key parameter. This dependence is far from being fully understood in the general case, but useful correlations, more empirical than theoretical, have been formulated for a few types of bridging ligands: hydroxo,[2] halides,[3,4] carboxylates,[5] azide and thiocyanate,[6] or even purine bases.[7]

The work presented here follows the research line that has been carried out in the last few years by our group on the interaction of 1,2,4-triazolo[1,5-*a*]pyrimidine ligands with metal ions; a review about the subject has been recently published by us.[8] These compounds present several positions in their molecules for binding metal ions making them suitable for building dinuclear or polynuclear compounds. The interactions between the metal centres have been studied by means of molecular orbital (MO) calculations in dimeric compounds of silver(I)[9] and platinum(II),[10] but dinuclear copper(II) complexes with bridging triazolopyrimidine ligands have not been described previously to this article, despite the structural and theoretical interest of copper dinuclear compounds and their magnetic properties.

We describe here the synthesis and characterization of several copper(II) dinuclear complexes with the ligand 4,5-dihydro-5-oxo[1,2,4]triazolo[1,5-*a*]pyrimidine in its anionic form ($5tpO^-$) bridging the metal centres. The aim of this work is to characterize the bridging coordination behaviour of the ligand towards $Cu^{II}$, studying the relationship between the structure and the experimental properties of the isolated compounds. The role of the ligand has been determined by X-ray diffraction, an unexpected binding mode having been found in the compound with phenanthroline as

---

[a] Departamento de Química Inorgánica, Facultad de Ciencias, Universidad de Granada,
18071 Granada, Spain
Fax: (internat.) + 34-958/248526
E-mail: mquiros@ugr.es

[b] Grupo de Modelización y Diseño Molecular, Instituto de Biotecnología, Facultad de Ciencias, Universidad de Granada, 18071 Granada, Spain

[c] Departamento de Ciencia de los Materiales e Ingeniería Metalúrgica y Química Inorgánica, Facultad de Ciencias, Universidad de Cádiz,
Apartado 40, 11510 Puerto Real, Cádiz, Spain

[†] Professor José Molina Molina passed away on June 13, 2000.

1434−1948/02/0404−0811 $ 17.50+.50/0

an auxiliary ligand. The way in which the structural features influence the redox properties (observed by electrochemical measurements) and the intermetallic interaction (observed by magnetic susceptibility and EPR measurements) has been studied. The nature of this interaction has been theoretically analyzed by means of MO calculations for the compound with a quadruple bridge. The study of the formation process in solution of the related mono- and dinuclear complexes containing phenanthroline as an auxiliary ligand has revealed the role of the solvent.

## Results and Discussion

The compounds described in this work are the following: $[Cu_2(5tpO)_4(H_2O)_2]{\cdot}2H_2O$, (**1**) $[Cu_2(phen)_2(5tpO)_2(H_2O)_2](NO_3)_2{\cdot}4H_2O$ (**2**), $[Cu_2(biim)_2(5tpO)_2(H_2O)](ClO_4)_2{\cdot}5.5H_2O$ (**3**), $[Cu_2(CH_3CO_2)_2(5tpO)_2\ (H_2O)_2]$ (**4**), and $[Cu(phen)(5HtpO)_2](NO_3)_2$ (**5**), 5HtpO being the ligand 4,5-dihydro-5-oxo[1,2,4]triazolo[1,5-*a*]pyrimidine and phen and biim representing respectively the auxiliary chelating ligands 1,10-phenanthroline and bisimidazole.

### Description of the Structures

The crystal structures of compounds **1**, **2**, and **3** have been determined from single-crystal X-ray diffractometry. The molecular structure of these compounds is depicted in Figures 1, 2, and 3. The three complexes are dinuclear with the anionic form of ($5tpO^-$) acting as the bridging ligand; four such bridges are present in compound **1** and two in compounds **2** and **3**. Attached to each copper atom in the two latter compounds, there is a bidentate aromatic amine (1,10-phenanthroline or 2,2′-bisimidazole) acting as an auxiliary ligand. A typical 4+1 square pyramidal environment (not considering the other copper atom) is completed by a water molecule at a longer distance (see Table 1) at the apical position, except for one of the metal atoms (Cu2) in compound **3**, which is square planar. Copper atoms are, in all cases, deviated from the corresponding basal planes away from their counterparts: the corresponding distances (also included in Table 1) seem to be influenced both by the presence of the water molecule in the fifth position (the deviation is almost zero for the square planar Cu atom and is higher when the $Cu-OH_2$ distance is shorter) and also by the proximity of the other metal atom. Nitrate **2** or perchlorate **3** ions balance the charge and non-coordinated water molecules complete the crystal structures.

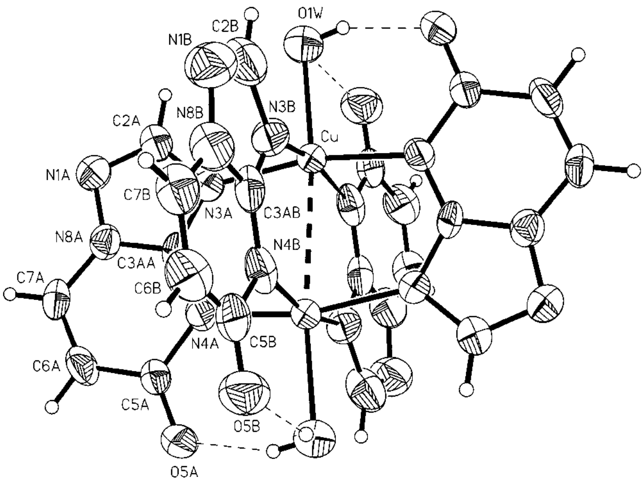

Figure 1. View of the molecular structure of compound **1**; atoms are represented as 50% probability thermal ellipsoids

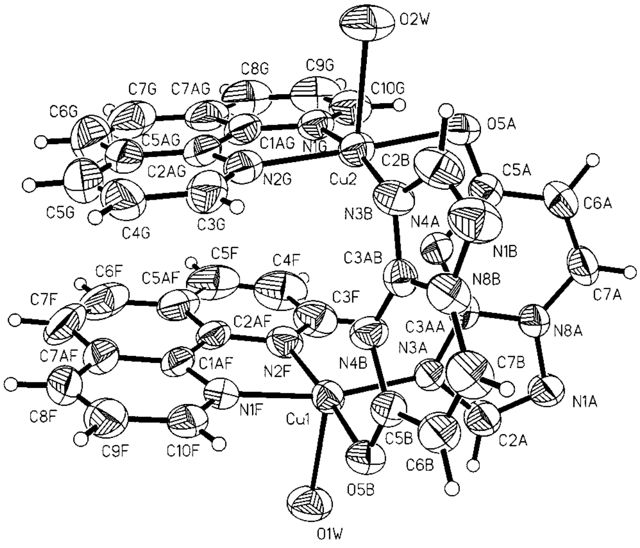

Figure 2. View of the molecular structure of compound **2**; atoms are represented as 50% probability thermal ellipsoids

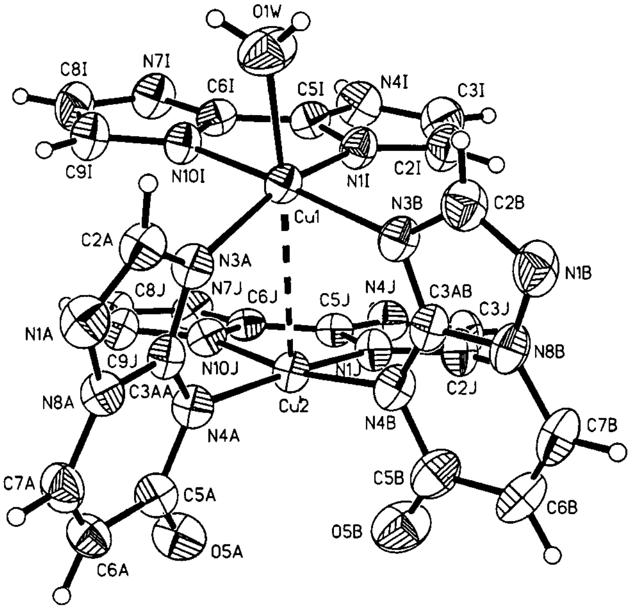

Figure 3. View of the molecular structure of compound **3**; atoms are represented as 50% probability thermal ellipsoids

The most outstanding feature of these structures is the different coordinating behaviour of the ligand. In **1** and **3**, the $5tpO^-$ entities bridge the metal atoms through the nitrogen atoms at positions 3 and 4; such a binding mode is

Table 1. Selected distances [Å] and angles [°]

| | 1 | 2 | 3 |
|---|---|---|---|
| Cu−Cu | 2.891(2) | 4.610(1) | 3.1968(7) |
| Cu−N3 | 2.000(8) | 2.004(6) | 1.994(3) |
| | 1.985(9) | 1.997(6) | 2.001(3) |
| Cu−N4 | 2.036(7) | − | 1.987(3) |
| | 2.080(9) | | 2.003(3) |
| Cu−O5 | − | 2.005(5) | − |
| | | 1.993(5) | |
| Cu−N(amine) | − | 2.009(6) | 2.005(3) |
| | | 2.012(6) | 2.020(3) |
| | | 2.010(6) | 1.995(3) |
| | | 2.028(7) | 2.018(3) |
| Cu−O(water) | 2.207(7) | 2.287(5) | 2.193(3) |
| | | 2.345(6) | |
| C5−O5 | 1.242(11) | 1.273(8) | 1.249(5) |
| | 1.217(13) | 1.280(8) | 1.240(6) |
| Cu−$N_4$/$N_3O$ plane | 0.2523(13) | 0.088(3) | 0.2599(10) |
| | | 0.080(3) | 0.0051(10) |
| N3−Cu−N3 | 87.0(4) | − | 91.30(13) |
| N4−Cu−N4 | 90.3(3) | − | 93.11(13) |
| N3−Cu−N4 *cis* | 88.4(3) | − | − |
| | 90.7(3) | | |
| N3−Cu−N4 *trans* | 165.5(3) | − | − |
| | 165.4(3) | | |
| N3−Cu−O5 | − | 91.1(2) | − |
| | | 92.5(2) | |
| C3A−N4−C5 | 118.1(8) | 116.4(6) | 118.2(3) |
| | 115.5(9) | 116.7(6) | 118.5(4) |
| N4−C3A−N8 | 123.6(8) | 123.6(7) | 122.6(4) |
| | 124.0(10) | 123.9(7) | 122.7(4) |
| N4−C5−O5 | 120.5(8) | 117.0(7) | 119.1(4) |
| | 117.3(11) | 116.8(7) | 118.9(4) |

common for triazolopyrimidine ligands and has been observed for $Cu^{I}$,[11] $Ag^{I}$,[9,12] $Pd^{II}$,[13] $Pt^{II}$ [10] and heterometallic $Pt^{II}-Pd^{II}$ compounds,[14] but it was observed first for $Cu^{II}$, although other ligands such as purines interact with $Cu^{II}$ in a similar fashion.[15] The coordination behaviour of the ligand in **2**, is much more unusual, however, in using the exocyclic oxygen atom (instead of N4) together with N3 to bridge the metal atoms (Figure 2). We have not found any other example in the bibliography of this binding mode for any metal and any bicyclic aromatic heterocycle containing an exocyclic oxygen atom, apart from a compound with a single xanthinato ion bridging three titanium atoms in a disposition that is, however, rather different to that in our compound.[16]

The versatility of triazolopyrimidine ligands for binding metal ions has been well established in previous works[8] and the possible involvement of the exocyclic oxygen atom in coordination was predicted for $5tpO^{-}$ from theoretical calculations.[17] However, it is quite unexpected to find such different ligand binding modes for compounds that are otherwise so similar, and we cannot see a clear reason for this behaviour. Perhaps it is just a matter of crystal packing optimization or small differences between the stacking properties (or even just the steric demands) of both auxiliary ligands. These are not parallel but convergent in **2** and divergent in **3** as we move away from the metal atoms (angles between the average planes are 10.7 and 11.7°, respectively). Stacking interactions are possibly responsible for this, since the optimum stacking distance between parallel aromatic rings is around 3.4 Å,[18] intermediate between the intermetallic distance in compounds **2** and **3**.

There are also differences in the relative disposition of the ligands: it is head-head-tail-tail for **1**, head-tail for **2**, and head-head for **3**. The molecular symmetry is then $C_{2h}$ for **1**, $C_2$ for **2**, and $C_s$ for **3**. This symmetry is only local, however: the only exact crystallographic symmetry present in the dimers is the inversion centre in **1**. The relative disposition of the ligands in **1** is stabilized by the presence of the coordinated water molecule (see Figure 1) which forms strong hydrogen bonds with the carbonyl oxygen atoms of the ligands [distances O1W···O5, 2.651(10) and 2.689(12) Å] and is the same as that found in the analogous $Pt^{II}$ compound with 4,7-dihydro-5-methyl-7-oxopyrimidine.[10] Compounds analogous to **1** have been reported with purine ligands[15,19,20] and 7-azaindolate[21] and all of them present the $C_{2h}$ atropisomer. We have not found any example of a copper(II) compound similar to **3,** but the analogous $Pd^{II}$ complexes with 4,7-dihydro-5-methyl-7-oxopyrimidine[13] display head-tail geometry.

Bond lengths within the ligands are not significantly different from those in free 5HtpO,[17] except for the C5−O5 bond in **2**, which is somewhat longer as a consequence of O5 binding to the metal [1.236(3) Å for 5HtpO]. The bond angles within the ligands are very similar in the three compounds and differ from the values in free 5HtpO mainly in the angles around N4, C3A−N4−C5 being closed and N4−C3A−N8 being open [the angles in the free ligand are 122.6(2) and 118.8(2)° respectively].

The structures are stabilized by extensive hydrogen bonding, with water molecules being the donors towards carbonyl oxygen atoms, oxygen atoms of the anions and other water molecules. The nitrogen atoms of bisimidazole away from the copper atoms in **3** remain protonated and form hydrogen bonds in a "chelating" way towards the oxygen atom of a water molecule (N4I and N7I) and a neighbouring carbonyl oxygen (N4J and N7J). This suggests that these couples of atoms, if deprotonated, could act as new chelating binding sites for metal atoms.

## Infrared Spectra

The infrared spectrum of **5**, with the ligand in neutral form, is almost identical to that of the free ligand, displaying an intense band in the C=O region at 1684 $cm^{-1}$, with two shoulders at 1711 and 1738 $cm^{-1}$. The spectra of the other compounds, with the ligand in anionic form, display the expected shift of this band to lower wavenumber. The spectrum shows a single narrow band at 1649 $cm^{-1}$ for **1** and **3** and 1637 $cm^{-1}$ for **2**, this extra shift being perhaps due to the involvement of O5 in coordination. For compound **4**, the C=O band seems to overlap with a band of the acetate anion, giving rise to a broader band centred at 1640 $cm^{-1}$. The presence of the anions is indicated by the typical stretching vibrations of nitrate (**2** and **5**) and perchlorate (**3**) at 1385 and 1107 $cm^{-1}$ respectively. Assignment of other bands is quite uncertain.

### Studies in Solution of Compounds 2 and 5

The behaviour in solution of compound **2** and the related mononuclear compound **5** has been studied. Compound **2** has been chosen because of its greater solubility in water and the possibility of making useful comparisons with **5**. The visible spectrum of a $10^{-3}$ M aqueous solution of **2** presents a band centred at 670 nm ($\varepsilon = 72$) whereas for **5** the maximum appears at 710 nm ($\varepsilon = 38$). The spectra of the latter are identical to those of solutions containing $Cu^{II}$, 5HtpO, and phen in 1:1:1 molar ratio. These results seem to indicate that the dimeric structure of **2** is kept in solution or, at least, that **5** is not its decomposition product.

In order to explore the formation process of compounds **2** and **5**, kinetic studies were carried out using a stopped-flow apparatus. In these studies two solutions were mixed, one containing $Cu^{II}$ and phenanthroline at $10^{-3}$ M concentration each, and the other containing 5HtpO in concentrations ranging from $5 \cdot 10^{-3}$ to $10^{-2}$ M. When water or acetonitrile were used as the solvent, the mononuclear complex $[Cu(5HtpO)_2(phen)]^{2+}$ was generated within the stopped-flow mixing time without further spectral changes. Formation of the binuclear complex **2** was only observed if a mixed solvent (water/acetonitrile, 1:1) was used; in that case, the absorbance changes last for ca. 2 seconds. These results reveal an important effect of the solvent on the course of the reaction, in agreement with the synthetic procedures of **2** and **5** (see below), despite the fact that compound **2**, once obtained, seems to be stable in solution (see above). Unfortunately, a more detailed kinetic study of the formation of **2** was not possible because of the small absorbance changes and the overlap with the deviations of the stopped-flow baseline caused by the use of the mixed solvent.

### Electrochemical Studies

The electrochemical properties of complexes **1**, **2**, **3**, and **5** were studied by measuring their cyclic voltammograms (CV) and square-wave voltammograms (SWV) in aqueous solution. Solubility of compounds **1** and **3** in water is quite low, just enough to record the voltammograms; the even lower solubility of compound **4** precluded reliable measurements. Despite their binuclear nature, a single reduction signal is observed in the CV of **1**, **2**, and **3**. The corresponding reduction potentials are 0.49 V (**1**), 0.24 V (**2**), 0.20 V (**3**), and 0.27 V (**5**). The same is observed in the SWV of **1** and **3**, a single signal at the same potentials as the CV. On the other hand, the SWV of **2** shows two overlapping peaks at 0.239 and 0.293 V, which can be considered as indicative of the presence of two copper centres and as evidence that the binuclear structure is maintained in solution, as was also suggested by visible spectroscopy. In contrast, both the mononuclear compound **5** and the solution containing $Cu^{II}$, 5HtpO, and phen (1:1:1) show a single reduction peak close to 0.28 V. Controlled-potential coulometry confirmed that this signal corresponds to a single electron process. The possibility of a breakage of the dimeric compound to generate a mononuclear compound analogous to the cationic complex of **5** and a species of the type $[Cu(phen)(H_2O)_n]^{2+}$ can be ruled out by the absence of a reduction peak around 0.174 V in the voltammograms of **2**, which is what is observed in solutions containing only $Cu^{II}$ and phenanthroline.[22]

A comparison of the redox potential of the complexes $[Cu_2(5tpO)_2(phen)_2]$ or $[Cu(5HtpO)_2(phen)]^{2+}$ with those found for binary copper−phenanthroline complexes[22] indicates that the triazolopyrimidine ligand stabilizes $Cu^{I}$, probably by the generation of dimeric species analogous to the very stable ones formed by $Ag^{I}$ with these types of ligands.[12] This stabilization is corroborated by the quite high potential value obtained for **1** and for solutions containing $Cu^{II}$ and a great excess of 5HtpO (also 0.49 V).

### Magnetic Susceptibility Measurements and EPR Spectra

The magnetic susceptibility of the four compounds has been measured in the range 5−300 K. In this range, **2** behaves as a magnetically diluted compound obeying the Curie law with a constant effective magnetic moment of 1.86 BM. Thus, no interaction between the two copper atoms in the dimer is observed. As expected, the same happens for the mononuclear compound **5** with $\mu_{eff} = 1.95$ BM.

On the other hand, **1**, **3**, and **4** present a $\chi$ vs. $T$ curve with a maximum (Figure 4), indicative of antiferromagnetic interactions between the metal atoms. In the three cases, the data fit very well to the Bleaney−Bowers equation for copper(II) dimers.[23] The values of $g$ and $2J$ (energy gap between the singlet and the triplet state) obtained from this fit are shown in Table 2. The interaction is very strong for compounds **1** and **4** and fairly strong for **3**. The trend in the strength of the interaction **1** >> **3** >> **2** is the expected one according to the number of bridging ligands, the length of the path across the ligand and the Cu−Cu distance.

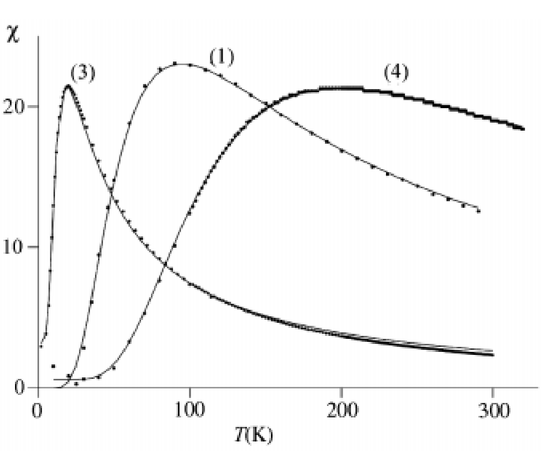

Figure 4. Magnetic susceptibility of compounds **1**, **3**, and **4** as a function of temperature; data (in emu/mol) have been multiplied by $5 \cdot 10^3$ (**1**), by $10^3$ (**3**), or by $10^4$ (**4**); solid lines represent the Bleaney−Bowers equation with the parameters indicated in Table 2

Table 2. Data from magnetic susceptibility measurements and EPR spectra

| | 1 | 3 | **4** |
|---|---|---|---|
| From $\chi$ measurements | | | |
| g | 2.148 | 2.081 | 2.117 |
| $2J$ [cm$^{-1}$] | $-104.9$ | $-21.6$ | $-221.3$ |
| From EPR spectra: | | | |
| $g_{\parallel}$ | 2.28 | ca. 2.3 | 2.36 |
| $g_{\perp}$ | 2.05 | 2.05 | 2.06 |
| $D$ [cm$^{-1}$] | 0.161 | 0.095 | 0.247 |

The value of $2J$ in **1** is, however, considerably smaller than those found in compounds with quadruple purine bridges,[7] including that with the adeninate anion,[24] which is the most similar one. The wide range of values found for these compounds indicate how sensitive $2J$ is to subtle changes in the structure. We have not been able to find a clear and unambiguous relationship between $2J$ and any structural parameter.

The interaction in **4** is even stronger than in **1**, the value of $2J$ being intermediate between that of the latter and that of the copper acetate dimer ($2J = -305$ cm$^{-1}$).[25] We have not been able to grow crystals of compound **4** large enough to undergo X-ray determination, but these data allow us to propose a molecular dimeric structure with two acetate and two 5tpO$^{-}$ bridging ligands, with the two water molecules occupying apical positions.

X-band EPR spectra have been recorded for the polycrystalline powdered samples at room temperature. Compound **2** presents a spectrum made up by a single very broad asymmetric band with an average $g$ value of 2.11, which could be attributed to an unresolved anisotropic triplet or doublet spectrum. No half-field transition is detected for this compound. The mononuclear compound **5** presents a normal axial spectrum with $g_{\parallel} = 2.25$ and $g_{\perp} = 2.08$.

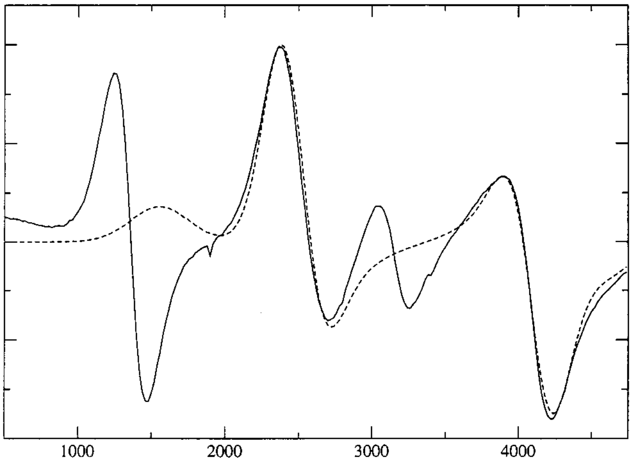

Figure 5. Experimental (———) and simulated (- - -) X-band EPR spectra of **1**; the simulation does not include the $S = 1/2$ and the half-field transitions (features at 3200 and 1400 G); simulation parameters, collected in Table 2, also reproduce well the Q-band spectrum; the spectrum of compound **4** is analogous to this

The other three spectra are quite complex and their main features have been assigned to ($S = 1$, $\Delta M_S = 1$) transitions with axial symmetry, although the parallel components in the spectrum of **3** are quite broad and difficult to identify. Together with these, strong signals also appear assignable to $S = 1/2$ transitions and, in the case of **1** and **4**, there is also a quite strong half-field ($S = 1$, $\Delta M_S = 2$ transition) band. As all these features overlap, the Q-band spectrum was also recorded for **1** to help in the assignments. Using computer simulation by means of the WINEPR program,[26] the values in Table 2 were finally obtained. Figure 5 displays the experimental and the calculated X-band spectra for **1**, only the ($S = 1$, $\Delta M_S = 1$) transitions are included in the simulation, which easily explains the differences between both. It is noteworthy that, comparing the zero-field splitting parameters of these compounds, we find the same trend as when comparing the $2J$ values.

### Theoretical Studies

In order to analyze the Cu···Cu interaction in **1**, theoretical calculations have been performed for the singlet state of this compound. Its geometry was optimized and constrained to $C_{2h}$ symmetry (thus, keeping a mirror plane that relates "head" with "head" and "tail" with "tail" and a binary axis perpendicular to it, so that the four ligands are equivalent). A very good agreement between the experimental and theoretical geometries was obtained; in particular, the theoretical Cu···Cu distance obtained was 2.893 Å. As in previous work by our group,[27] the hybrid density functional method with a large basis set (B3LYP/6-311G*) has been demonstrated to be accurate for describing large transition-metal complexes.

The topology of the electron charge density $\rho(r)$ was analyzed by means of the "Atoms in Molecules" (AIM) theory.[28,29] This analysis revealed the presence of a bond critical point (BCP) between the metal atoms, showing that the corresponding atomic basins share a common surface, and thus supporting the existence of a direct metal−metal interaction. As a consequence, four ring critical points (RCP) also appear at the middle of the Cu−Cu−C−N−C irregular pentagons. The $\rho(r)$ value at the Cu−Cu BCP is 0.012 $ea_o^{-3}$, only about one eighth of the corresponding values at the Cu−N bonds (0.085 and 0.081 $ea_o^{-3}$); this value may be taken as a rough estimation of the strength of the interaction. The Laplacian of the electron density [$\nabla^2(\rho)$] is positive at both Cu−Cu and Cu−N BCP (with values 0.054, 0.344, and 0.302 $ea_o^{-5}$ for Cu−Cu, Cu−N3, and Cu−N4 respectively), as expected for closed-shell types of interactions, which are always found in coordination bonds and metal-metal interactions.

It is interesting to have a look at the shape of the calculated MO of the compound, particularly the HOMO and the LUMO, which are displayed in Figure 6. Looking only at one half of these orbitals, they resemble the antibonding combination of the $d_{x^2-y^2}$ orbital of the metal atom and the proper symmetry adapted combination of the orbitals of the ligands, as expected from textbook simple MO theory for metal complexes. These two halves mix with each other

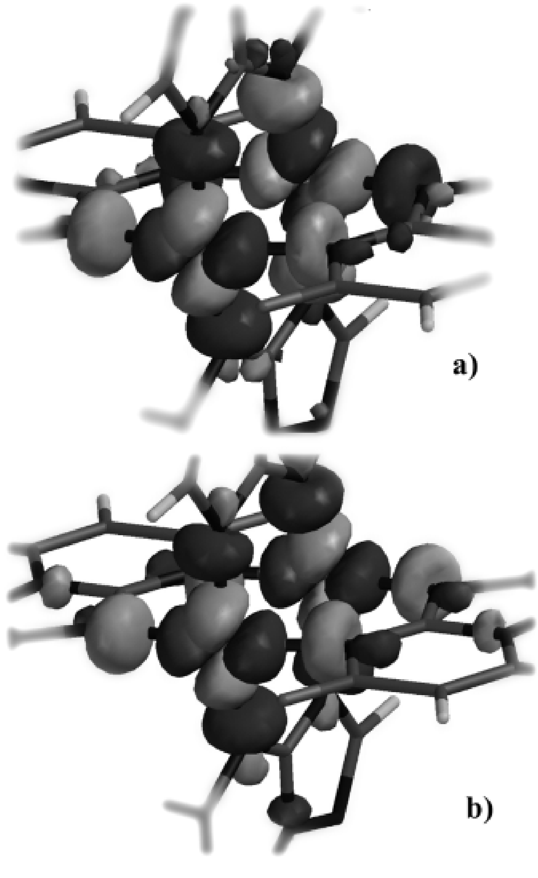

Figure 6. Calculated (B3LYP/6-311G*) HOMO (a) and LUMO (b) of **1**

giving rise to a "same-phase" ($b_g$) and to a "opposite-phase" ($a_u$) combination, the latter (HOMO) with less energy than the former (LUMO). The fact that the lobes of the HOMO on one copper atom have opposite signs to those on the other copper atom indicates that this orbital is antibonding (Δ antibonding) for the Cu−Cu union. This result, surprising at first sight, indicates that the stabilization of the HOMO with respect to the LUMO does not come from the direct intermetallic interaction, but from energetically more favourable electronic distribution within the ligands.

The calculated energy gap between these two orbitals is 1.095 eV, which of course cannot be regarded, not even as a first approximation, as the energy difference between the singlet and the triplet state. This latter value ($2J$) can only be theoretically obtained by performing separate calculations for both states (singlet and triplet) and subtracting the corresponding total energies. Extremely accurate methods must be applied for this since the goal is to get a small number by subtracting another two, very similar to each other and several orders of magnitude larger. Nevertheless, a method for calculating $2J$ in copper(II) dimers has been developed by Ruiz et al.,[30] which implies performing a so-called "broken-symmetry" calculation for the singlet state without geometry optimization (that is, keeping the geometry observed by X-ray data). This method has yielded good results for some systems[31] but the assumption that the energy of the singlet is well represented by the broken-symmetry model has been criticized by several authors.[32,33] Nevertheless, we have tested the method with our compound but the results do not reproduce, even qualitatively, the experimental data.

## Conclusions

In this work, we have demonstrated the ability of the ligand 4,5-dihydro-5-oxo[1,2,4]triazolo[1,5-*a*]pyrimidinate ($5tpO^-$) to bridge copper(II) atoms to form dimeric species. Four such compounds have been isolated, three of them having been structurally characterized by single-crystal X-ray diffraction: compound **1** with a quadruple bridge and compounds **2** and **3** with a double bridge, and containing phenanthroline or bisimidazole, respectively, as auxiliary ligands. The bridging mode of the ligand in **1** and **3** is the one most usually found in the triazolopyrimidine ligand through the nitrogen atoms in positions 3 and 4, whereas compound **2** displays an unprecedented binding mode trough N3 and the exocyclic oxygen atom. The dimeric nature of compound **4**, for which X-ray structural data are not available, is indicated by its magnetic behaviour and EPR spectrum, which allow us to tentatively propose the presence of two $5tpO^-$ and two acetate bridges.

The structural features of these compounds clearly influence their electrochemical, magnetic and EPR properties. Thus, the ligand ability for stabilizing lower oxidation states is indicated by the reduction potentials, which increase with the number of $5tpO^-$ ligands attached to the metal. The dimeric nature of **1**, **3**, and **4** is shown by their strong antiferromagnetic behaviour as well as by their triplet EPR spectra, these methods not showing clearly the interaction for the compound with the longer bite (**2**). Opposite to this, the SWV of **2** display a double peak, probably revealing its dimeric nature in solution, whereas the reduction of $Cu^{II}$ to $Cu^{I}$ seems to be simultaneous for both metal atoms in **1** and **3**.

The strength of the intermetallic interaction, measured as the $2J$ parameter, is clearly correlated with the number and nature of bridging ligands and with the length of the bite, following the order: **4** > **1** > **3** > **2**. For compound **1**, an unsuccessful attempt has been made for calculating this parameter theoretically. The zero-field splitting of the triplet state, as deduced from the EPR spectra, follows the same trend as $2J$.

A theoretical analysis has been performed by means of MO calculations for compound **1**. The calculated geometry fits well with the experimental one and the Bader analysis indicates the existence of a direct contact between the metal basins (the BCP). The topology of the HOMO of the compound indicates that its stabilization with respect to the LUMO comes from the electronic structure within the ligands rather than from the direct intermetallic interaction.

Lastly, it is interesting to note the need for a mixed solvent for the formation of compound **2**, revealed by kinetic measurements, in agreement with the synthetic procedure.

## Experimental Section

### Synthesis of the Compounds

4,5-dihydro-5-oxo[1,2,4]triazolo[1,5-*a*]pyrimidine (5HtpO) was synthesized as indicated in a previous work.[17] Bisimidazole was also synthesized according to the literature.[34] Copper salts, other reagents and solvents were obtained from standard commercial suppliers.

**$[Cu_2(5tpO)_4(H_2O)_2]\cdot 2H_2O$ (1):** A suspension was made with 80 mg (0.24 mmol) of copper basic carbonate and 200 mg (1.47 mmol) of 5HtpO in 20 mL of water, the mixture being stirred at room temperature for 30 min. After this, a dark blue precipitate was obtained, which was dissolved by adding 10 mL of acetonitrile to the mixture. Unchanged copper carbonate was then filtered off and, after two days of keeping the solution at room temperature, dark blue crystals of **1** were obtained. Yield: 40 mg (7.4%). $C_{20}H_{20}Cu_2N_{16}O_8$: calcd. C 32.48, H 2.71, N 30.31; found C 32.68, H 2.79, N 30.52%.

**$[Cu_2(phen)_2(5tpO)_2(H_2O)_2](NO_3)_2\cdot 4H_2O$ (2):** 240 mg (1 mmol) of copper(II) nitrate trihydrate and 180 mg (1 mmol) of 1,10-phenanthroline (phen) were dissolved in 20 mL of methanol. This solution was mixed with another one containing 136 mg (1 mmol) of 5HtpO in 20 mL of water/acetonitrile 2:1. After one week, blue crystals of the compound appeared. Yield: 300 mg (30%). $C_{34}H_{34}Cu_2N_{14}O_{14}$: calcd. C 41.25, H 3.43, N 19.82; found C 41.45, H 3.23, N 19.96%.

**$[Cu_2(biim)_2(5tpO)_2(H_2O)](ClO_4)_2\cdot 5.5H_2O$ (3):** The same procedure was followed as for compound **2**, using copper(II) perchlorate hexahydrate instead of copper(II) nitrate and 2,2′-bisimidazole (biim) instead of 1,10-phenanthroline. Yield: 50 mg (5.2%). $C_{22}H_{29}Cl_2Cu_2N_{16}O_{15.5}$: calcd. C 27.47, H 3.04, N 23.31; found C 27.66, H 3.09, N 23.50%.

**$[Cu_2(CH_3CO_2)_2(5tpO)_2(H_2O)_2]$ (4):** The procedure starts as for compound **1**, but the dark blue solid initially obtained is treated with 20 mL of a 10% solution of acetic acid in ethanol instead of acetonitrile, which dissolves it completely. After two days, a blue microcrystalline solid was obtained. Yield: 50 mg (12.5%). $C_{14}H_{16}Cu_2N_8O_8$: calcd. C 30.49, H 2.92, N 20.32; found C 30.62, H 3.13, N 20.21%.

**$[Cu(phen)(5HtpO)_2](NO_3)_2$ (5):** 240 mg (1 mmol) of copper(II) nitrate trihydrate and 180 mg (1 mmol) of 1,10-phenanthroline (phen) were dissolved in 20 mL of acetonitrile. 272 mg (2 mmol) of 5HtpO were then added and the suspension was refluxed for 30 min, after which the product was obtained as a blue powder. Yield: 500 mg (78%). $C_{22}H_{16}CuN_{12}O_8$: calcd. C 41.31, H 2.52, N 26.29; found C 41.34, H 2.44, N 26.54%.

**Instrumental Work:** Microanalysis of C, H and N were performed in a Fisons Instruments EA-1008 analyzer, X-band EPR spectra were recorded in a X-band Bruker ESP-300 apparatus (all this equipment sited at the Centre of Scientific Instrumentation of the University of Granada). The Q-band spectrum of **1** was recorded on a Q-band Bruker ESP-300 apparatus. IR spectra were obtained using a FT MIDAC Prospect 1 spectrophotometer with samples dispersed in KBr pellets. Magnetic susceptibility measurements were made in a SQUID MPMS-XL Quantum Design magnetometer. Solution electronic spectra were obtained using a Perkin−Elmer Lambda 3B spectrophotometer, whereas the stopped-flow experiments were carried out using an Applied Photophysics SX 17MV instrument.

**X-ray Crystallography:** X-ray work was carried out at room temperature on a Stoe Stadi4 (**1** and **2**) or Siemens P4 (**3**) diffractometer with Mo-$K_\alpha$ radiation. The dimensions of the chosen crystals were (in mm) 0.6 × 0.3 × 0.1 (**1**), 0.45 × 0.3 × 0.15 (**2**), and 0.5 × 0.4 × 0.3 (**3**). Data collections were performed in $2\Theta/\omega$ scan mode. The number of independent reflections collected were, after averaging, 3908, 7333, and 4640 for **1**, **2**, and **3**, respectively. Data were corrected for Lorentz and polarization effects and empirically (psi-scans) for absorption (transmission ranges: 0.5888−0.6927 for **1**, 0.6456−0.7601 for **2**, and 0.6471−0.7750 for **3**). The structures were solved by standard Patterson methods and refined by full-matrix least-squares using the SHELXL-93[35] (**1**, **2**) or SHELXL-97[36] (**3**) programs. One of the nitrate ions and two water molecules in **2** were found to be disordered over two positions, as well as two water molecules in compound **3**; another water molecule in this compound was refined with an occupancy of 1/2. Fixed N−O distances (1.19 Å) were imposed to the disordered nitrate. Atoms with an occupancy of less than one were refined isotropically, all other non-hydrogen atoms were refined anisotropically. Hydrogen atoms of the organic residues were introduced in their ideal positions, those of water molecules were found and refined with a fixed O−H distance (0.86 Å) in

Table 3. Crystal and refinement data for compounds **1**, **2**, and **3**

| | 1 | 2 | 3 |
|---|---|---|---|
| Empirical formula | $C_{20}H_{20}Cu_2N_{16}O_8$ | $C_{34}H_{34}Cu_2N_{14}O_{14}$ | $C_{22}H_{29}Cl_2Cu_2N_{16}O_{15.5}$ |
| Molecular mass | 739.60 | 989.83 | 963.59 |
| Space group | Pbca | $P2_1/c$ | $P\bar{1}$ |
| *a* [Å] | 10.2473(5) | 11.957(2) | 11.6132(9) |
| *b* [Å] | 16.1318(8) | 14.422(3) | 12.2274(8) |
| *c* [Å] | 16.2087(12) | 23.888(4) | 14.7856(12) |
| α [deg] | − | − | 97.278(7) |
| β [deg] | − | 104.13(1) | 108.381(6) |
| γ [deg] | − | − | 110.615(6) |
| *V* [Å$^3$] | 2679.4(3) | 3994.5(12) | 1796.8(2) |
| Z | 4 | 4 | 2 |
| $\rho_{calcd.}$ [g/cm$^3$] | 1.833 | 1.646 | 1.781 |
| μ [mm$^{-1}$] | 1.67 | 1.15 | 1.43 |
| $R_1$(F) [$F_o^2 > 2\sigma(F_o^2)$] | 0.1138 | 0.0718 | 0.0391 |
| $R_w(F_o^2)$ (all data) | 0.2631 | 0.1879 | 0.1062 |
| CCDC deposition number | 160636 | 160637 | 160638 |

compounds **1** and **3** and were not found in compound **2**. An isotropic thermal parameter was applied to all hydrogen atoms 1.2 times those of their parent atoms. The full sets of crystal data (excluding structure factors) for these compounds have been deposited with the Cambridge Crystallographic Data Centre (CCDC, 12 Union Road, Cambridge CB2 1EZ, UK, E-mail: deposit@ccdc.cam.ac.uk), the corresponding deposition numbers are indicated in Table 3, together with selected crystal data.

**Electrochemical Measurements:** The electrochemical measurements were carried out using an EG&G PARC model 163A potentiostat provided with a Pt disk working electrode and a Pt wire auxiliary electrode. A Ag/AgCl electrode was used as reference for the measurements in water and the measured potentials were referenced to the normal hydrogen electrode by adding 0.222 V.[37] The complex solutions for electrochemical measurements (1−2 mM) contained 0.10 M $KNO_3$ and were purged with $N_2$ and thermostated at 25.01°C before measurement. The CVs were recorded at a scan rate of 50 mV/s and the SWVs with a frequency of 5 Hz.

**MO and Electronic Charge Density Calculations:** Density functional theory (B3LYP) calculations were performed with the Gaussian 98 package of programs.[38] The singlet state of structure **1** was fully optimized at the B3LYP/6-311G* level, with constrained $C_{2h}$ symmetry and tested with frequency calculations (no imaginary frequencies). The Bader analysis was made by using the AIMPAC series of programs,[39] with the DFT density as input as described in the AIM theory.[28,29]

Calculations at the B3LYP/6-31G* level without geometry optimization have also been performed for both the singlet and the triplet state, including for the singlet state the "broken-symmetry" procedure that has been described elsewhere[30] in order to get an estimate for the $2J$ value.

## Acknowledgments

This work was supported by a DGES project (PB 97-0786-CO3) from Ministerio de Educación y Cultura. Computing time was provided by the Universidad de Granada. We are grateful to Professor R. F. W. Bader for a copy of the AIMPAC package of programs. We acknowledge Professors T. Rojo and J. L. Lezama (Universidad del País Vasco) for collecting the Q-band spectrum of compound **1** and help with its assignment. We are also grateful to Professor R. Sáez (Universidad Autónoma de Madrid) for the magnetic measurements. M. Abul Haj acknowledges UNESCO for a PEACE grant.

---

[1] M. Melník, M. Kabešová, M. Koman, L. Macášková, J. Garaj, C. E. Holloway, A. Valent, *J. Coord. Chem.* **1998**, *45*, 147−359.

[2] V. H. Crawford, H. W. Richardson, J. R. Wasson, D. J. Hodgson, W. E. Hatfield, *Inorg. Chem.* **1976**, *15*, 2107−2110.

[3] W. E. Marsh, K. C. Patel, W. E. Hatfield, D. J. Hodgson, *Inorg. Chem.* **1983**, *22*, 511−515.

[4] M. A. Romero, J. M. Salas, M. Quirós, M. P. Sánchez, J. Romero, D. Martín, *Inorg. Chem.* **1994**, *33*, 5477−5481.

[5] E. Colacio, M. Ghazi, R. Kivekäs, J. M. Moreno, *Inorg. Chem.* **2000**, *39*, 2882−2890.

[6] J. A. R. Navarro, M. A. Romero, J. M. Salas, M. Quirós, E. R. T. Tiekink, *Inorg. Chem.* **1997**, *36*, 4988−4991.

[7] D. Sonnenfroh, R. W. Kreilick, *Inorg. Chem.* **1980**, *19*, 1259−1262.

[8] J. M. Salas, M. A. Romero, M. P. Sánchez, M. Quirós, *Coord. Chem. Rev.* **1999**, *193*, 1119−1142.

[9] M. A. Romero, J. M. Salas, M. Quirós, M. P. Sánchez, J. Molina, J. El Bahraoui, R. Faure, *J. Mol. Struct.* **1995**, *354*, 189−195.

[10] J. A. R. Navarro, M. A. Romero, J. M. Salas, M. Quirós, J. El Bahraoui, J. Molina, *Inorg. Chem.* **1996**, *35*, 7829−7835.

[11] J. G. Haasnoot, T. L. F. Favre, W. Hinrichs, J. Reedijk, *Angew. Chem. Int. Ed. Engl.* **1988**, *27*, 856−857.

[12] J. A. R. Navarro, J. M. Salas, M. A. Romero, R. Faure, *J. Chem. Soc., Dalton Trans.* **1998**, 901−904.

[13] J. A. R. Navarro, M. A. Romero, J. M. Salas, *J. Chem. Soc., Dalton Trans.* **1997**, 1001−1005.

[14] J. A. R. Navarro, M. A. Romero, J. M. Salas, M. Quirós, *Inorg. Chem.* **1997**, *36*, 3277−3283.

[15] A. Terzis, A. L. Beauchamp, R. Rivest, *Inorg. Chem.* **1973**, *12*, 1166−1170.

[16] A. L. Beauchamp, F. Belanger-Gariepy, A. Mardhy, D. Cozak, *Inorg. Chim. Acta* **1986**, *124*, L23−L24.

[17] M. Abul Haj, J. M. Salas, M. Quirós, J. Molina, R. Faure, *J. Mol. Struct.* **2000**, *519*, 165−172.

[18] W. Saenger, *Principles of Nucleic Acid Structure*; Springer-Verlag; New York, **1984**.

[19] P. de Meester, A. C. Skapski, *J. Chem. Soc. A* **1971**, 2167−2169.

[20] E. Sletten, *Acta Crystallogr., Sect. B* **1970**, *26*, 1609−1614.

[21] S. M. Peng, Y. N. Lin, *Acta Crystallogr., Sect. C* **1986**, *42*, 1725−1731.

[22] C. J. Hawkins, D. D. Perrin, *J. Chem. Soc.* **1962**, 1351−1357.

[23] B. Bleaney, K. D. Bowers, *Proc. Royal Soc. London Ser. A* **1952**, 451−465.

[24] R. W. Duerst, S. J. Baum, G. F. Kokoszka, *Nature* **1969**, *222*, 665−666.

[25] R. J. Doedens, *Prog. Inorg. Chem.* **1976**, *21*, 209−231.

[26] *WINEPR SimFonia*, version 1.25 (shareware version). Bruker Analytische Messtechnick GmbH, **1996**.

[27] J. A. Dobado, R. Uggla, M. R. Sundberg, J. Molina, *J. Chem. Soc., Dalton Trans.* **1999**, 489−496.

[28] R. F. W. Bader, *Atoms in Molecules: a Quantum Theory*; Clarendon Press: Oxford, 1990.

[29] R. F. W. Bader, *Chem. Rev.* **1991**, *91*, 893−928.

[30] E. Ruiz, P. Alemany, S. Álvarez, J. Cano, *J. Am. Chem. Soc.* **1997**, *119*, 1297−1303.

[31] I. Castro, M. L. Calatayud, J. Sletten, F. Lloret, J. Cano, M. Julve, G. Seitz, K. Mann, *Inorg. Chem.* **1999**, *38*, 4680−4687.

[32] R. Caballol, O. Castell, F. Illas, P. R. Moreira, J. P. Mabrieu, *J. Phys. Chem. A* **1997**, *101*, 7860−7866.

[33] C. Adam, V. Barone, A. Bencini, F. Totti, I. Ciofini, *Inorg. Chem.* **1999**, *38*, 1996−2004.

[34] F. Holmes, K. M. Jones, E. G. Torrible, *J. Chem. Soc.* **1961**, 4790−4795.

[35] G. M. Sheldrick, SHELXL 93. *Program for the Refinement of Crystal Structures.* University of Göttingen, Germany, **1993**.

[36] G. M. Sheldrick, SHELXL 97. *Program for the Refinement of Crystal Structures.* University of Göttingen, Germany, **1997**. Available at http://shelx.uni-ac.gwdg.de/SHELX/.

[37] N. Navon, G. Golub, H. Cohen, P. Paoletti, B. Valtancoli, A. Bencini, D. Meyerstein, *Inorg. Chem.* **1999**, *38*, 3484−3488.

[38] M. J. Frisch, G. W. Trucks, H. B. Schlegel, G. E. Scuseria, M. A. Robb, J. R. Cheeseman, V. G. Zakrzewski, J. A. Montgomery, Jr., R. E. Stratmann, J. C. Burant, S. Dapprich, J. M. Millam, A. D. Daniels, K. N. Kudin, M. C. Strain, O. Farkas, J. Tomasi, V. Barone, M. Cossi, R. Cammi, B. Mennucci, C. Pomelli, C. Adamo, S. Clifford, J. Ochterski, G. A. Petersson, P. Y. Ayala, Q. Cui, K. Morokuma, D. K. Malick, A. D. Rabuck, K. Raghavachari, J. B. Foresman, J. Cioslowski, J. V. Ortiz, B. B. Stefanov, G. Liu, A. Liashenko, P. Piskorz, I. Komaromi, R. Gomperts, R. L. Martin, D. J. Fox, T. Keith, M. A. Al-Laham, C. Y. Peng, A. Nanayakkara, C. González, M. Challacombe, P. M. W. Gill, B. Johnson, W. Chen, M. V. Wong, J. L. Andrés, C. González, M. Head-Gordon, E. S. Replogle, J. A. Pople, *GAUSSIAN 98, revision A.4.* Gaussian, Inc., Pittsburgh PA, **1998**.

[39] F. W. Biegler-König, R. F. W. Bader, T.-H. Tang, *J. Comput. Chem.* **1982**, *3*, 317−328.

Received April 17, 2001
[I01133]